

Effect of Extended Tooth Contact on the Modeling of Spur Gear Transmissions

Hsiang Hsi Lin & Jifeng Wang
 Memphis State University
 Memphis, TN

Fred B. Oswald & John J. Coy
 NASA Lewis Research Center
 Cleveland, OH

Abstract

In some gear dynamic models, the effect of tooth flexibility is ignored when the model determines which pairs of teeth are in contact. Deflection of loaded teeth is not introduced until the equations of motion are solved. This means the zone of tooth contact and average tooth meshing stiffness are underestimated, and the individual tooth load is overstated, especially for heavily loaded gears.

This article compares the static transmission error and dynamic load of heavily loaded, low-

contact-ratio spur gears when the effect of tooth flexibility has been considered and when it has been ignored. Neglecting the effect yields an underestimate of resonance speeds and an overestimate of the dynamic load.

Introduction

It is well known that the dynamics of gear systems can be influenced considerably by the stiffness of the meshing gear teeth (Refs. 1-5). A principal excitation for gear dynamics and vibration is the variation of this stiffness caused by teeth entering and leaving mesh. This stiffness variation is a primary cause of the time-varying component of static transmission error. The static transmission error is defined as relative displacement of the driving gear with respect to the driven gear along the line of action. The static transmission error also can be affected by gear errors such as tooth profile and spacing, runout, alignment and deflection under load.

An important task for developing a gear dynamic model is the determination of which pairs of teeth actually are in contact at any instant. In some models, the gear teeth are treated as rigid when contact conditions are determined (Refs. 3, 4, 6-9). However, in an actual transmission, the load-carrying teeth deform elastically. This causes the incoming tooth pair to enter contact earlier than the theoretical start of contact. Similarly, the loaded outgoing teeth will leave contact later than the theoretical end of contact. This extends the

Nomenclature

E_d	gear error due to tooth deflection, mm (in)
E_s	tooth spacing error, mm (in)
E_p	tooth profile error or profile modification, mm (in)
E_t	static transmission error of gear pair, mm (in)
K_g	stiffness of gear mesh, N/mm (lb/in)
Q^a, Q^b, Q^c	meshing compliance of tooth pairs a, b and c , mm/N (in/lb)
R_{a1}, R_{a2}	addendum radii of gear 1 and gear 2, mm (in)
R_{b1}, R_{b2}	base radii of gear 1 and gear 2, mm (in)
R_1, R_2	pitch radii of gear 1 and gear 2, mm (in)
S_a, S_r	separation distance in approach and recess, mm (in)
W	total static transmitted load, N (lb)
W^a, W^b, W^c	static transmitted load on tooth pairs a, b , and c , N (lb)
Δ_1	separation angle: rotation of gear 1 (gear 2 fixed), rad
Δ_2	separation angle: rotation of gear 2 (gear 1 fixed), rad
Subscripts:	
j	contact point of meshing tooth pair
1	driving gear
2	driven gear

tooth contact zone and increases the average mesh stiffness.

In this article the effect of extended tooth contact on heavily loaded spur gears is examined. The static transmission error and dynamic load were calculated for gears of moderate contact ratio (1.64) as well as for somewhat higher contact ratio (1.95). The calculated results were compared to evaluate the influence of extended tooth contact on the static and dynamic loads of a low-contact-ratio spur gear transmission. The findings may form the basis for improvements in the spur gear dynamic analysis code DANST (Dynamic ANALYSIS of Spur gear Transmissions).

Theory and Analysis

Two sets of low-contact-ratio gears were considered for an analytical study. The two sets are the same except for the tooth addendum, which was adjusted to provide contact ratios of 1.64 and 1.95. Parameters for the gears are given in Table 1. The analyses were performed using the NASA gear dynamic code DANST. The analytical procedures are described in the following sections.

Gear System Model

Fig. 1 shows a four-degree-of-freedom, lumped-mass model for a typical gear transmission. The model includes driving and driven gears, connecting shafts, motor and load. The equations of motion were derived from basic gear geometry and elementary vibration principles. The dynamic process is studied in the rotating plane of the gears, and gear tooth contact is assumed to be along the line of action. The model and differential equations of motion are described in more detail in Refs. 10 and 11.

Meshing Stiffness and Transmission Error (Neglecting Extended Tooth Contact)

To study the static transmission error and meshing stiffness of a low-contact-ratio gear system, we designate three consecutive tooth pairs — a , b and c — and begin our analysis at the moment in which pair a is carrying the entire load (single contact zone) and tooth pair b is just about to enter contact. The initial contact of tooth pair b occurs at the point where the addendum circle of the driven gear intersects the line of action. At this instant, double contact begins. As the gears rotate, the point of contact moves along the line of action. When

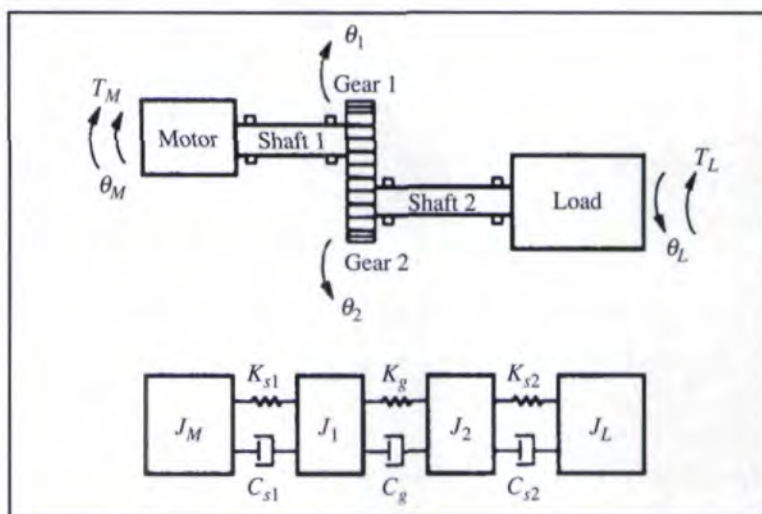


Fig. 1 — Gear transmission model.

tooth pair b reaches the theoretical point of transition between double and single contact, the leading tooth pair a disengages, leaving only pair b in single contact. When tooth pair b reaches the next theoretical transition point for single and double contact, tooth pair c comes into contact and begins to share the load (double contact); thus, the meshing action alternates between double and single contact zones as the gears rotate.

To investigate the effect of tooth flexibility on the zone of tooth contact, we will examine in detail the first double tooth contact zone (where tooth pairs a and b are in contact). With these two tooth pairs in contact, the static transmission error E_t and the shared tooth load W_j for each individual tooth pair at contact point j may be expressed as:

$$(E_t^a)_j = (E_{d1}^a)_j + (E_{d2}^a)_j + (E_{p1}^a)_j + (E_{p2}^a)_j \quad (1)$$

$$(E_t^b)_j = (E_{d1}^a)_j + (E_{d2}^b)_j + (E_{p1}^b)_j + (E_{p2}^b)_j + (E_{s1}^b)_j + (E_{s2}^b)_j \quad (2)$$

$$W = W_j^a + W_j^b \quad (3)$$

The tooth spacing errors above are determined with reference to tooth pair a (which is therefore assumed to have no spacing error). These spacing errors are due to manufacturing. The error terms are expressed as linear displacements along the line of action. The static transmission error E_t is the total relative displacement of the driven gear with respect to the driving gear along this line. As long as they are both in contact, the static transmission error of tooth pairs a and b must be the same. There-

Dr. Hsiang Hsi Lin

is associate professor of mechanical engineering at Memphis State University. He is a member of ASME and AGMA.

Jifeng Wang

is a doctoral candidate at Memphis State University. He previously studied at the Research Academy of Mechanical Engineering and the Northeast Heavy Machinery Institute, People's Republic of China.

Fred B. Oswald

is a research engineer at NASA Lewis Research Center. He is the author of more than 20 papers on gear and transmission subjects and is a member of ASME.

Dr. John J. Coy

is the branch chief, mechanical systems technology, NASA Lewis Research Center. He is the author of more than 80 technical papers on gearing and related subjects.

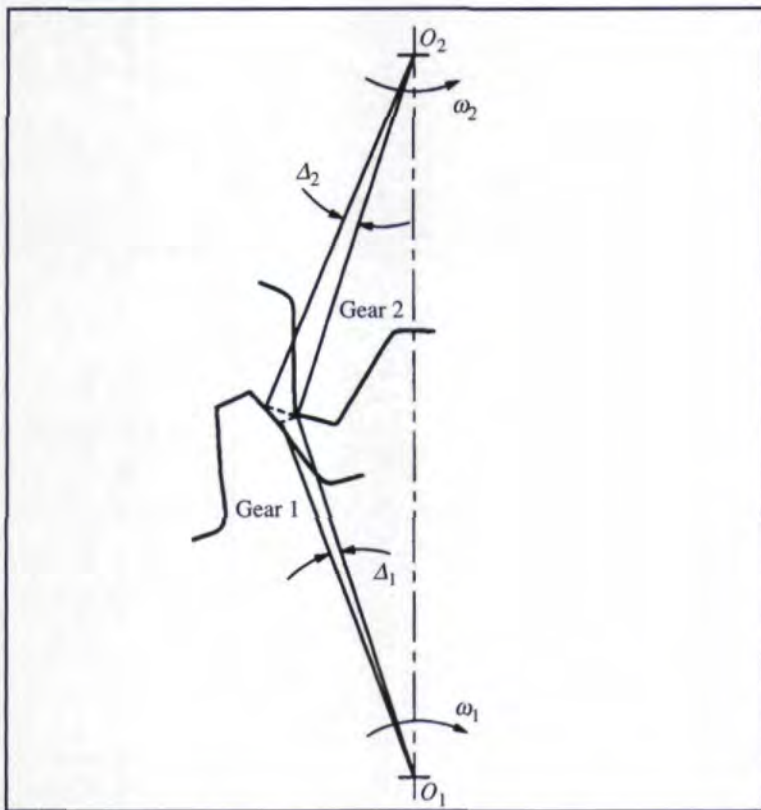


Fig. 2 — Separation angles of a tooth pair in approach.

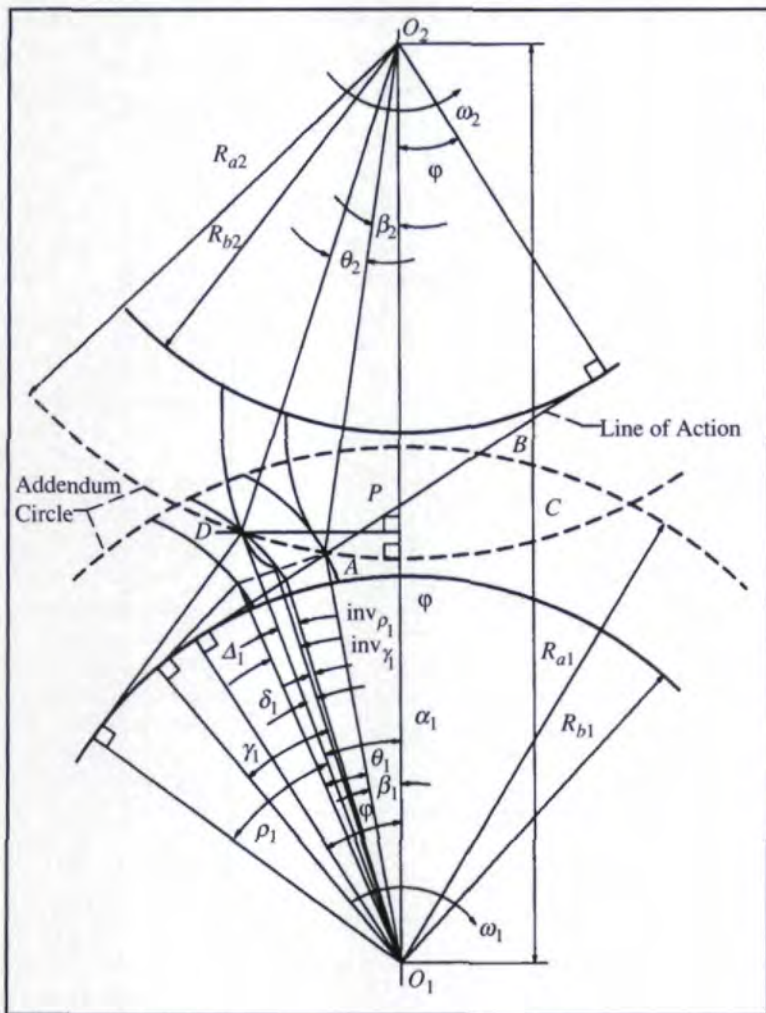


Fig. 3 — Separation distance calculation for a tooth pair in approach (gear 2 fixed).

fore, from Eqs. 1 – 3,

$$Q_j^a W_j^a + (E_p^a)_j = Q_j^b W_j^b + (E_p^b)_j + (E_s^b)_j \quad (4)$$

where

$$(E_s)_j = (E_{s1})_j + (E_{s2})_j \quad (5)$$

$$(E_p)_j = (E_{p1})_j + (E_{p2})_j \quad (6)$$

$$(E_d)_j = (E_{d1})_j + (E_{d2})_j = Q_j W_j \quad (7)$$

The gear meshing stiffness K_g at contact point j is then

$$(K_g)_j = \frac{W_j^a}{(E_t^a)_j} + \frac{W_j^b}{(E_t^b)_j} \quad (8)$$

In the analyses above and those to follow, the position of the contact point j on the gear teeth is expressed in terms of the roll angle of the driving gear tooth. In the single contact zone, the transmission error and meshing stiffness equations are much simpler and can be derived by similar procedures.

Gear Teeth Separation Distance

We define the tooth separation distance as the distance between a pair of teeth just out of contact during approach or recess if there is no elastic deformation. This distance, expressed along the line of action, is equal to the product of separation angle and base radius of the gear. The separation distance will be compared with the static transmission error to determine the contact condition.

To calculate the separation distance, we introduce the separation angle (exaggerated for clarity in Fig. 2) for a pair of teeth (pair b) in approach, where gear 1 represents the driving gear and gear 2 the driven gear. The separation angle is not the same for the two mating gears. Δ_2 is the angular rotation required for gear 2 to close the gap between the teeth of pair b . Likewise, Δ_1 is the required rotation of gear 1 while gear 2 is held stationary. The actual tooth contact will start at a point where the separation angle of the incoming tooth pair is equal to the angular deflection of the preceding tooth pair(s).

The equations for the separation distance as a function of the separation angle can be

derived for a tooth pair in approach using Fig. 3. In Fig. 3, the driven gear (gear 2) is regarded as fixed. Point *A* represents the theoretical start of contact of a tooth pair, point *B* the theoretical end of contact, and point *P* the pitch point, when no load is applied. To find the separation angle Δ_1 , the two gears were rotated backward to a position just before contact at θ_1 and θ_2 , respectively. The tooth pair will make contact at point *D* if the elastic deformation of the preceding tooth pair(s) caused the driving gear (gear 1) to rotate an angle of Δ_1 . The equivalent separation distance along the line of action, S_1 , between the incoming tooth pair due to the rotation of gear 1 can be found from:

$$S_1 = \Delta_1 R_{b1} \quad (9)$$

where

$$\Delta_1 = \theta_1 + \beta_1 - \alpha_1 + \delta_1 \quad (10)$$

$$\theta_1 R_1 = \theta_2 R_2 \quad (11)$$

$$\delta_1 = \text{inv } \rho_1 - \text{inv } \gamma_1 \quad (12)$$

$$\beta_1 = \tan^{-1} \left(\frac{R_{a2} \sin \beta_2}{C - R_{a2} \cos \beta_2} \right) \quad (13)$$

$$\beta_2 = \cos^{-1} \left(\frac{R_{b2}}{R_{a2}} \right) - \phi \quad (14)$$

$$\alpha_1 = \tan^{-1} \left(\frac{R_{a2} \sin (\theta_2 + \beta_2)}{C - R_{a2} \cos (\theta_2 + \beta_2)} \right) \quad (15)$$

$$\rho_1 = \cos^{-1} \left(\frac{R_{b1}}{DO_1} \right) \quad (16)$$

$$\gamma_1 = \cos^{-1} \left(\frac{R_{b1}}{AO_1} \right) \quad (17)$$

$$DO_1 = \sqrt{[R_{a2} \sin (\theta_2 + \beta_2)]^2 + [C - R_{a2} \cos (\theta_2 + \beta_2)]^2} \quad (18)$$

$$AO_1 = \sqrt{[R_{a1} \sin \beta_2]^2 + [C - R_{a2} \cos \beta_2]^2} \quad (19)$$

Similar expressions can be derived for the linear separation distance S_2 , where gear 1 is fixed and gear 2 rotates to close the gap. Likewise, expressions can be derived for the separation distances S_1 and S_2 of a tooth pair in recess, where S_1 and S_2 are defined for tooth pair *a*.

Fig. 4 shows the variation of the separation distance during approach and recess as a function of the rotation angle (θ_1 in Fig. 3) for a 1:1 ratio gear pair as described in Table 1 and with contact ratio 1.64. The zero rotation angle in the abscissa refers to the gear position at the theoretical start (or end) of tooth contact in approach (or recess). The separation distances S_1 and S_2 differ, and the difference grows larger as the rotation angle increases. The magnitude of S_1 is less than S_2 in approach and greater than S_2 in recess. Since there is no particular reason to consider either the driving or the driven gear to be fixed, an average value of S_1 and S_2 has been taken as the separation dis-

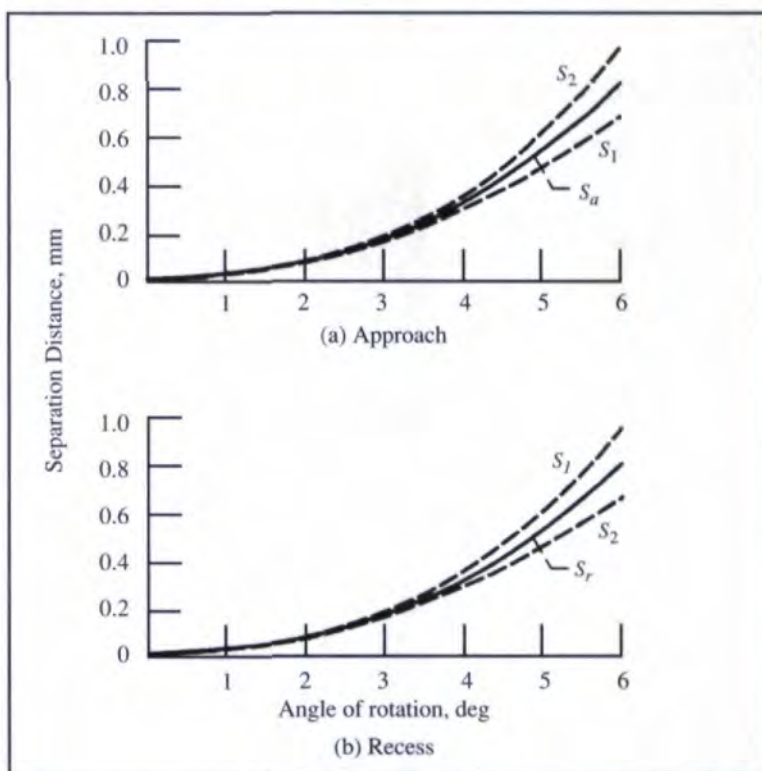


Fig. 4 — Separation distance calculated for approach and recess.

Table 1 — Sample Gear Parameters

Number of teeth.....	28, 28
Pressure angle, deg.....	20
Module, mm (diametral pitch, 1/in).....	3.18 (8)
Backlash, mm (in).....	0.05 (0.002)
Face width, mm (in).....	25.4 (1.00)
Design torque, N-m (lb-in).....	373 (3290)
Normalized tooth addendum.....	1.00 or 1.20
Theoretical contact ratio.....	1.64 or 1.95

tance. S_a is designated as the separation distance during approach and S_r is that for recess.

The computer program DANST was used to calculate the static transmission error for the gear system described in Table 1. To simplify the analysis, only unmodified gears are considered here. DANST is based on algorithms developed in Refs. 10 and 11.

Fig. 5(a) shows the theoretical (extended contact ignored) static transmission error for gears of contact ratio 1.64. The static transmission error consists of manufacturing errors added to the deflection due to load. In this study manufacturing errors, such as spacing and profile errors and runout, are neglected. This is a reasonable assumption for high-quality, heavily loaded gears; therefore, the static transmission error represents the elastic deflection of the gear teeth and gear blank. The horizontal axis in Fig. 5(b) is calibrated in terms of the roll angle for tooth b . This is the same as the rotation angle (used in Fig. 4) except for a constant offset.

Meshing Stiffness and Transmission Error (Including Extended Tooth Contact)

Superimposed on the transmission error curve in Fig. 5(a) are separation distance curves S_a and S_r . The actual point where the approaching tooth pair b makes contact is the point labeled C' , where the separation distance equals the static transmission error. Likewise, tooth pair a , in recess, leaves contact at the point labeled B' .

Five regions (designated I to V) are identified in Fig. 5(a). Regions I (AB) and V (CD) represent double contact zones; region III ($B'C'$) is the single contact zone; and regions II (BB') and IV ($C'C$) represent the increased double (or reduced single) contact regions due to the effect of tooth flexibility. This effect increases the contact ratio of the gear pair about 5% (from 1.64 to 1.72).

To evaluate the static transmission error of region II, we adopt an analysis similar to that presented above. We begin at the moment when tooth pair b is in contact at the point labeled B in Fig. 5(a). (This is the end of the theoretical double contact zone.) Elastic deflection causes tooth pair a to remain in contact until b reaches B' . The total transmitted load W shared by tooth pairs a and b in this region is:

$$W = \frac{(E_t^a)_j - (S_r^a)_j}{Q_j^a} + \frac{(E_t^b)_j}{Q_j^b} \quad (20)$$

where the first term at the right-hand side of the equation represents the load on tooth pair a , and the second term represents the load on tooth pair b at an arbitrary contact point j .

The static transmission error of all tooth pairs in contact must be equal; therefore, the transmission error of b in this region can be calculated from Ref. 13:

$$(E_t^b)_j = \frac{Q_j^b (S_r^a)_j + Q_j^a Q_j^b W}{Q_j^a + Q_j^b} \quad (21)$$

When E_t^b , the static transmission error of tooth pair b , is less than the separation distance, S_r^a , tooth pair a leaves contact. This occurs as tooth pair b reaches B' . (This is the beginning of region III, where b is the only tooth pair in

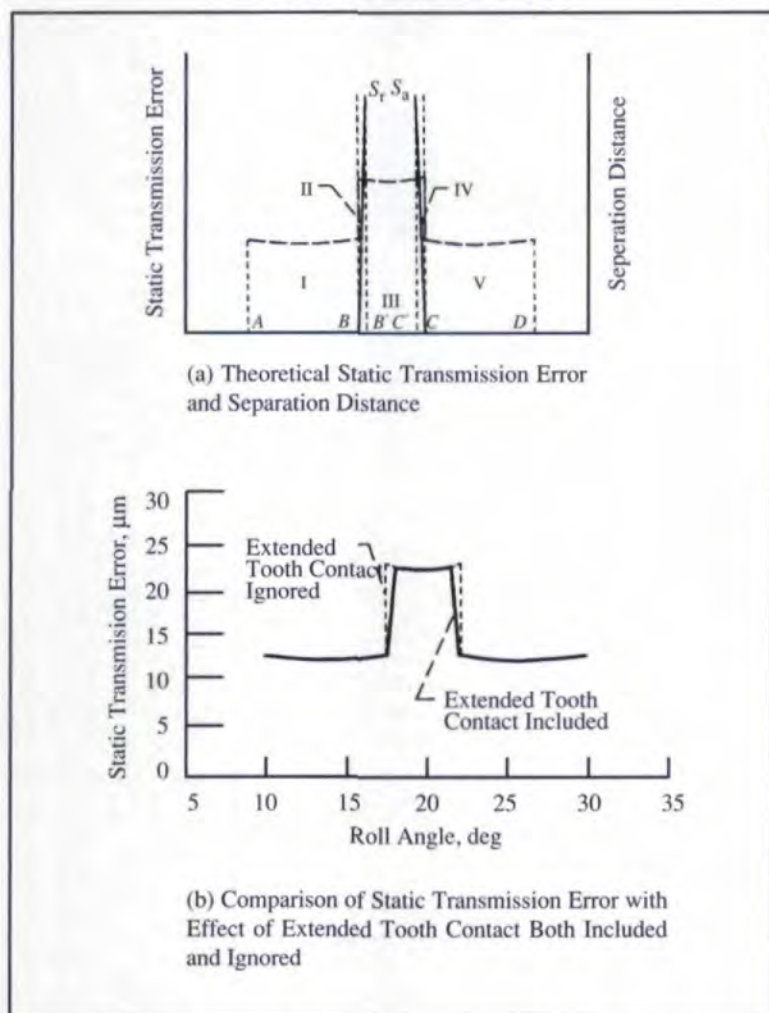


Fig. 5 — Static transmission error and separation distance for gears with contact ratio = 1.64.

contact.) The gears remain in single contact until tooth pair b reaches point C' .

At the beginning of region IV, when b arrives at point C' , tooth pair c engages and gradually increases its share of the total transmitted load. The shared tooth load and static transmission error of tooth pairs b and c change with respect to the rotation of gears. They can be determined from the following expressions:

$$W = \frac{(E_t^b)_j}{Q_j^b} + \frac{(E_t^c)_j - (S_a^c)_j}{Q_j^c} \quad (22)$$

$$(E_t^b)_j = \frac{Q_j^b(S_a^c)_j + Q_j^b Q_j^c W}{Q_j^b + Q_j^c} \quad (23)$$

Fig. 5(b) compares the transmission error calculated with extended tooth contact included (solid line) and ignored (dashed line).

If the tooth addendum (and hence the height of the teeth) is increased, the contact ratio becomes greater. The increase in the contact ratio reduces the zone of single contact. The width in the step in the static transmission error curve will be reduced as the separation distance curves S_a and S_r approach each other. These effects can be seen in Fig. 6(a).

If the theoretical contact ratio is increased to slightly less than 2.00, the increase in contact length due to extended tooth contact may cause the single contact zone to completely disappear. This is illustrated in Fig. 6(b), in which the tooth addendum of the gears was increased by 20% over the standard value to increase the theoretical contact ratio to 1.95. The actual contact ratio (after consideration of tooth flexibility) is 2.02.

Fig. 6(a) shows the static transmission error for the gears with theoretical contact ratio of 1.95. The single tooth contact zone (regions II to IV) is so narrow compared to regions I and V that the figure was plotted at an expanded scale. (Only portions of regions I and V are shown.) For regions I (AB) and V (CD), the static transmission error curve is similar to Fig. 5(a). Regions II (BC') and IV ($B'C$) are extended zones of double tooth contact (similar to the corresponding regions in Fig. 5(a)). The trans-

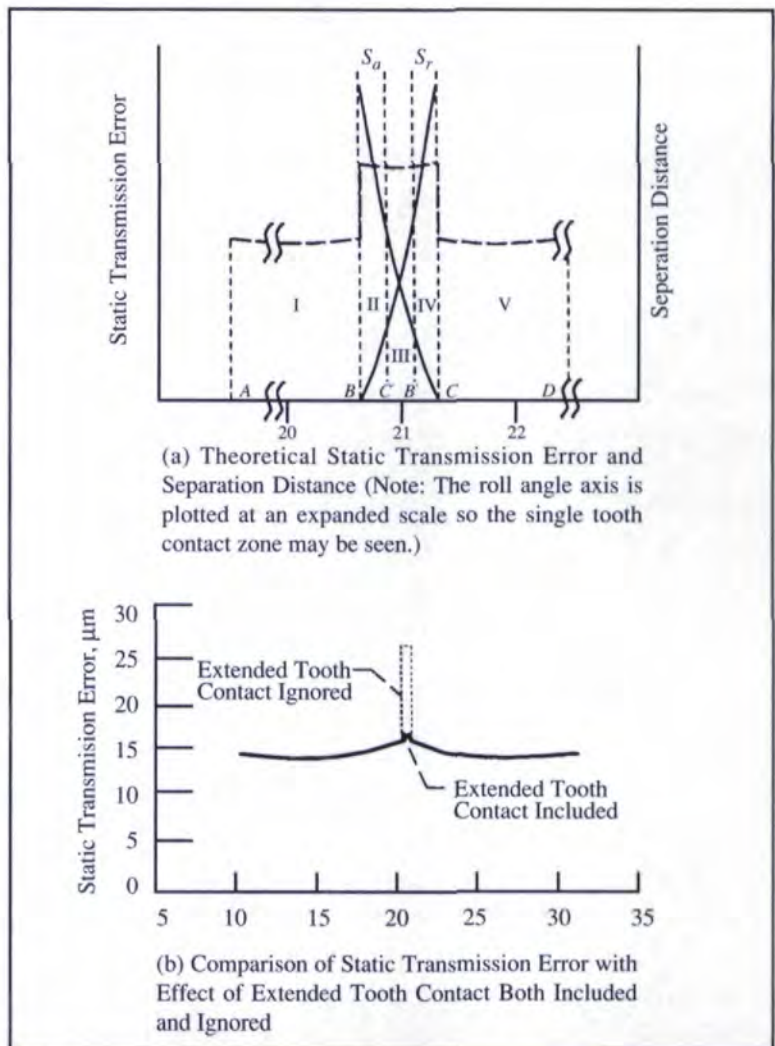


Fig. 6 — Static transmission error and separation distance for gears with contact ratio = 1.95.

mission error in these regions can be found from Eqs. 18-21 as in the previous case.

In region III ($C'B'$), tooth pair b is carrying most of the load, but pairs a and c are also in contact; hence, this is a triple contact zone. The transmitted load shared by the tooth pairs a , b and c is given by:

$$W = \frac{(E_t^a)_j - (S_r^a)_j}{Q_j^a} + \frac{(E_t^b)_j}{Q_j^b} + \frac{(E_t^c)_j - (S_a^c)_j}{Q_j^c} \quad (24)$$

The transmission error of the three tooth pairs in contact must be equal, therefore:

$$(E_t^b)_j = \frac{Q_j^a Q_j^b (S_a^c)_j + Q_j^b Q_j^c (S_r^a)_j + Q_j^a Q_j^b Q_j^c W}{Q_j^a Q_j^b + Q_j^b Q_j^c + Q_j^a Q_j^c} \quad (25)$$

In Fig. 6(b) the magnitude of the transmission error was significantly reduced because the single contact region was entirely eliminated.

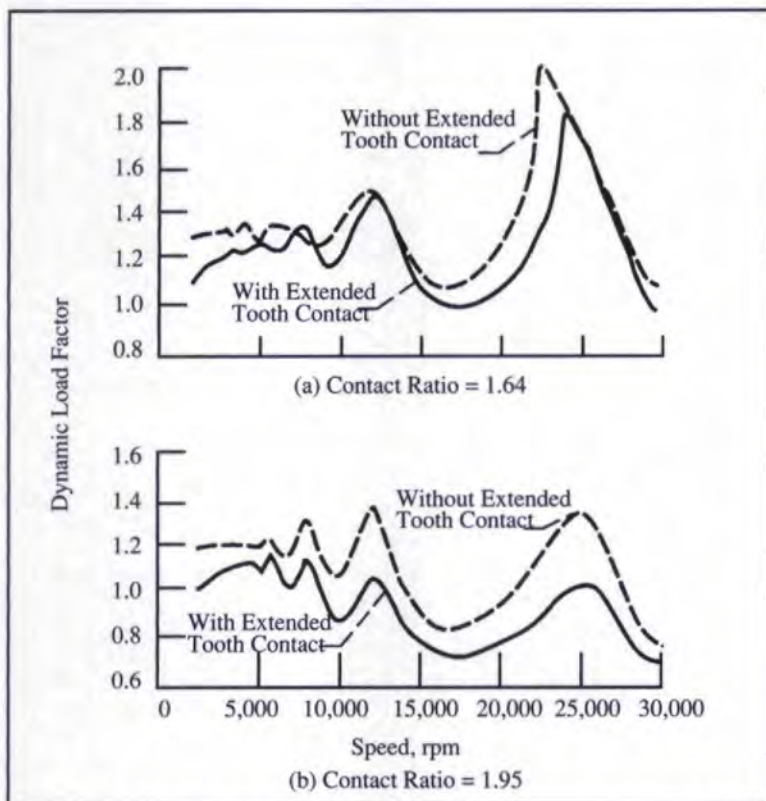


Fig. 7 — Predicted dynamic load factor of gears as a function of speed, with and without the effect of extended tooth contact.

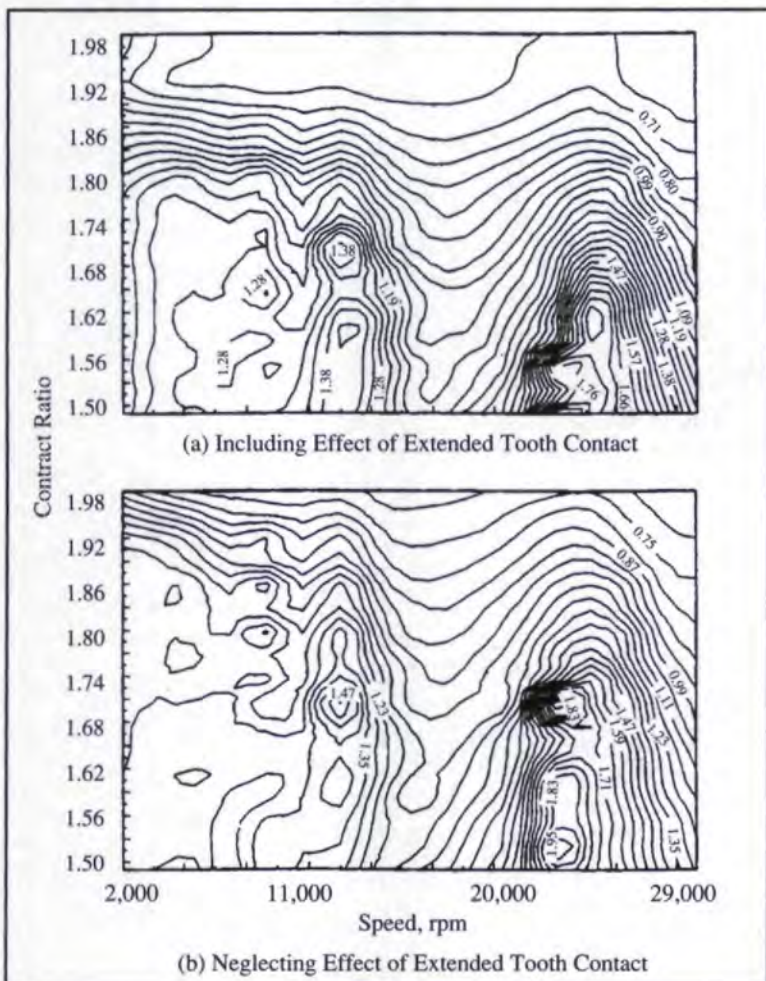


Fig. 8 — Predicted dynamic load factor of gears as a function of speed and contact ratio.

The predicted dynamic excitation of this gear pair will be similarly reduced from that calculated with the extended tooth contact neglected. The difference is greater for gears with a higher contact ratio (which generally have more flexible teeth), especially at heavy load.

Results and Discussion

DANST was used to calculate the dynamic load for our sample gear system. To compare the dynamic load predicted under different conditions, we define a non-dimensional term called the dynamic load factor. This is the ratio of the maximum dynamic load divided by the total static load. The total static load is the torque divided by the base circle radius. For gears with contact ratio greater than 2, the dynamic load factor may be less than 1.

Figs. 7(a) and (b) contain many individual solutions for the dynamic load factor arranged in the form of speed surveys. The speed surveys are shown two ways — with the effect of extended tooth contact neglected and included. Fig. 7(a) is for a set of sample gears with standard tooth addendum ($1/DP$). The theoretical contact ratio (neglecting extended tooth contact) is 1.64. The response of the gear system peaks at the resonant speed near 25,000 rpm. There are also smaller peaks at submultiples of the resonant speed.

Including extended tooth contact in the model increases the predicted system resonant speed from approximately 23,250 to 24,600 rpm, while the predicted dynamic load factor at resonance is reduced from about 2.02 to 1.84, a 9% reduction in dynamic load. Extended tooth contact results in greater load sharing (increasing the length of double or triple contact zones), which, in turn, increases the average mesh stiffness. Other effects include an increase in the system resonant speed and a reduction in the maximum dynamic load.

Fig. 7(b) illustrates the results for a set of gears with tooth addendum increased by 20% (to $1.2/DP$) over the standard value. This increases the theoretical contact ratio to 1.95. Including extended tooth contact in the analysis reduces the predicted dynamic factor at resonance from 1.42 to 1.10, a reduction of nearly 23%. Unlike the example above, there is little change in the predicted system resonant speed (25,000 rpm). Apparently, elimination of the very narrow single contact zone

(Fig. 6) has little effect on the average gear meshing stiffness.

Figs. 8(a) and (b) are contour plots which illustrate the effects of both speed and contact ratio on the predicted dynamic load factor. The speed was varied over the range 2,000 to 30,000 rpm, and the theoretical contact ratio was varied from 1.50 to 1.98. (As above, the contact ratio was varied by adjusting the tooth addendum.) These figures show how both factors affect spur gear dynamics.

Fig. 8(a) shows the predicted results if extended contact is neglected. The resonant response at 23,000 rpm shows the highest dynamic loads for contact ratios of 1.52 and 1.70. In Fig. 8(b) the analysis was repeated with extended tooth contact included. Fig. 8(b) shows an overall lower level of dynamic response than Fig. 8(a). The resonant response has shifted to about 25,000 rpm, and there is less effect from changes in the contact ratio.

Conclusions

The NASA gear dynamic code DANST was used for an analytical study of the influence of tooth flexibility to extend the zone of tooth contact for heavily loaded spur gears. This effect was both neglected and included as the static transmission error and dynamic load were calculated for low-contact-ratio spur gears. The following conclusions were drawn from the investigation:

1. Neglecting the extension of the contact zone results in underestimating resonant speeds and overestimating the dynamic load, especially for heavily loaded gears.

2. The effect is more significant for gears with a theoretical contact ratio nearly (slightly less than) 2.00. For these gears, the increased zone of tooth contact may extend the actual contact ratio beyond 2.00.

3. For the cases studied in this article, ignoring the effect results in an underestimate of the contact ratio by about 3 to 5%. ■

References:

1. Harris, S. L. "Dynamic Loads on the Teeth of Spur Gears." *Proceedings of the Institute of Mechanical Engineers*, Vol. 172, No. 2, 1958, pp. 87-112.
2. Terauchi, Y., H. Nadano and M. Nohara. "On the Effect of the Tooth Profile Modification on the Dynamic Load and the Sound Level of the Spur Gears." *JSME Bulletin*, Vol. 25, No. 207,

1982, pp. 1474-1481.

3. Cornell, R. W. and W. W. Westervelt. "Dynamic Tooth Loads and Stressing for High Contact Ratio Spur Gears." *ASME Trans., Journal of Mechanical Design*, Vol. 100, No. 1, 1978, pp. 69-76.
4. Lin, H. H., D. P. Townsend and F. B. Oswald. "Dynamic Loading of Spur Gears with Linear or Parabolic Tooth Profile Modifications." *Proc. of ASME 5th Int. Power Trans. and Gearing Conf.*, Chicago, IL, Vol. 1, 1989, pp. 409-419.
5. Tavakoli, M. S. and D. R. Houser. "Optimum Profile Modifications for the Minimization of Static Transmission Errors of Spur Gears." *ASME Trans., Journal of Mechanisms, Transmissions, and Automation in Design*, Vol. 108, Mar. 1986, pp. 86-95.
6. Yang, D. C. H. and Z. S. Sun. "A Rotary Model for Spur Gear Dynamics." *ASME Trans., Journal of Mech., Trans., and Automation in Design*, Vol. 107, Dec. 1985, pp. 529-535.
7. Vexlex, P. and D. Berthe. "Dynamic Tooth Loads on Geared Train." *Proc. of ASME 5th Int. Power Trans. and Gearing Conf.*, Chicago, IL, 1989, pp. 447-454.
8. Kubo, A. and S. Kiyono. "Vibration Excitation of Cylindrical Involute Gears." *JSME Bulletin*, Vol. 23, No. 183, Sept. 1980, pp. 1536-1543.
9. Terauchi, Y. and K. Nagamura. "On Tooth Deflection Calculation and Profile Modification of Spur Gear Teeth." *Int. Symp. on Gearing and Power Trans.*, Tokyo, Japan, 1981, pp. 159-164.
10. Lin, H. H., R. L. Huston and J. J. Coy. "On Dynamic Loads in Parallel Shaft Transmissions: Part I — Modelling and Analysis." *ASME J. of Mech., Trans., and Automation in Design*, Vol. 110, No. 2, 1988, pp. 221-225.
11. Lin, H. H., R. L. Huston and J. J. Coy. "On Dynamic Loads in Parallel Shaft Transmissions: Part II — Parameter Study." *ASME J. of Mech., Trans., and Automation in Design*, Vol. 110, No. 2, 1988, pp. 226-229.
12. Seager, D. L. "Separation of Gear Teeth in Approach and Recess, and the Likelihood of Corner Contact." *ASLE Trans.*, Vol. 19, No. 2, May 1975, pp. 164-170.
13. Tse, D. and H. H. Lin. "Separation Distance and Static Transmission Error of Involute Spur Gears." *AIAA Paper 92-3490, AIAA/SAE/ASME /ASEE 28th Joint Propulsion Conf.*, Nashville, TN, July 6-8, 1992.

Acknowledgement: Originally presented at the *AIAA/SAE/ASME/ASEE 29th Joint Propulsion Conference & Exhibit, 1993, Monterey, CA. Available as NASA Technical Memorandum 106174.*